

MS-I

N 67-19340

FACILITY FORM 002

(ACCESSION NUMBER)

44

(PAGES)

CK-82542

(NASA CR OR TMX OR AD NUMBER)

(THRU)

1

(CODE)

10

(CATEGORY)

Summary Report

PHOTOMIXING DEVICES

by

B. Emmons

Period Covered: 15 February 1965 to 15 February 1966

Date of Publication: 15 March 1966

Philco No. A045

NAS 8-5030

Prepared for

George C. Marshall Space Flight Center
National Aeronautics and Space Administration
Huntsville, Alabama



PHILCO

A SUBSIDIARY OF *Ford Motor Company*

APPLIED RESEARCH LABORATORY

Summary Report

PHOTOMIXING DEVICES

by

B. Emmons

Period Covered: 15 February 1965 to 15 February 1966

Date of Publication: 15 March 1966

Philco No. A045

NAS 8-5030

Prepared for

George C. Marshall Space Flight Center
National Aeronautics and Space Administration
Huntsville, Alabama

PHILCO.

A SUBSIDIARY OF *Ford Motor Company*

APPLIED RESEARCH LABORATORY
BLUE BELL, PENNSYLVANIA

TABLE OF CONTENTS

Section	Page
1 INTRODUCTION	1
2 TECHNICAL DISCUSSION	2
2.1 Theoretical Work	2
2.1.1 Noise in Avalanching Photodiodes	2
2.1.1.1 Case 1	3
2.1.1.2 Case 2	3
2.1.2 Frequency Response of Avalanching Photodiodes	5
2.2 Experimental Work	10
2.2.1 Material Studies	10
2.2.2 Guard-Ring Studies	11
2.2.3 Diode Fabrication and Testing	14
2.2.3.1 Fabrication	14
2.2.3.2 Testing	15
3 CONCLUSIONS AND RECOMMENDATIONS	35
4 LIST OF PUBLICATIONS	37
REFERENCES	38

LIST OF ILLUSTRATIONS

Figure		Page
1	Signal-to-Noise Ratio Versus Multiplication	6
2	Sketch of Proposed InAs Guard-Ring Diode	12
3	Reverse Bias Current — Voltage and Current Multipli- cation Characteristics for InAs-C10	16
4	Reverse Bias Current — Voltage and Current Multiplication Characteristics for InAs-C12	17
5	Reverse Bias Current — Voltage and Current Multiplication Characteristics for InAs-C14	18
6	Reverse Bias Current — Voltage and Current Multiplication Characteristics for InAs-C15	19
7	Reverse Bias Current — Voltage and Current Multiplication Characteristics for InAs-C16	20
8	Reverse Bias Current — Voltage and Current Multiplication Characteristics for InAs-C17	21
9	Reverse Bias Current — Voltage and Current Multiplication Characteristics for InAs-C18	22
10	Reverse Bias Current — Voltage and Current Multiplication Characteristics for InAs-C19	23
11	Reverse Bias Current — Voltage and Current Multiplication Characteristics for InAs-C20	24
12	Reverse Bias Current — Voltage and Current Multiplication Characteristics for InAs-C21	25
13	Reverse Bias Current — Voltage and Current Multiplication Characteristics for InAs-C22	26
14	Reverse Bias Current — Voltage and Current Multiplication Characteristics for InAs-C23	27

LIST OF ILLUSTRATIONS (Continued)

Figure		Page
15	Reverse Bias Current — Voltage and Current Multiplication Characteristics for InAs-C24	28
16	Reverse Bias Current — Voltage and Current Multiplication Characteristics for InAs-C25	29
17	Reverse Bias Current — Voltage and Current Multiplication Characteristics for InAs-C26	30
18	Reverse Bias Current — Voltage and Current Multiplication Characteristics for InAs-C27	31
19	Spectral Sensitivities of Multiplying InAs Diodes	33

SECTION 1

INTRODUCTION

This is the third summary report issued on Contract NAS 8-5030. It covers work done from 15 February 1965 to 15 February 1966.

The work described in this report was undertaken to obtain the experimental and theoretical information necessary to design and fabricate practical solid-state optical heterodyne detectors which display current gain.

The theoretical work was directed primarily toward determining the effect of current multiplication on diode bandwidth. In particular, the large influence of the ratio of the electron ionization coefficient to the hole ionization coefficient on the variation of bandwidth with multiplication is examined. Present knowledge of the excess noise associated with current multiplication is also summarized, and again, the important influence of the ratio of the electron ionization coefficient to the hole ionization coefficient is emphasized.

The experimental work was directed toward obtaining the largest possible current gain in InAs photodiodes, whose spectral response is most suitable for use with lasers in the 3-micron region.

Some attempts to correlate material quality with diode performance are discussed, and attempts to obtain a satisfactory guard-ring structure are reviewed. Finally, the construction and testing of a group of 16 diodes of the mesa type is described. These diodes represent the state-of-the-art at the close of the contract period. The diodes show a current multiplication of the order of 10 at 10 volts reverse bias. The RC cutoff frequencies of the diodes range from 0.3 to 1.7 GHz for diode areas in the range from 2.4 to $10 \times 10^{-4} \text{ cm}^2$.

SECTION 2

TECHNICAL DISCUSSION

2.1 THEORETICAL WORK

2.1.1 Noise in Avalanching Photodiodes

The use of avalanche multiplication as a possible means of raising the signal-power level at the output of a photodiode was suggested in February 1964.¹ For some time thereafter it was thought, and measurements indicated,^{2, 3} that the avalanche process would multiply both the signal and the noise power levels equally. Thus, little or no loss of signal-to-noise ratio at the diode output terminals was expected, and the device appeared to be a solid-state analog of the photo-multiplier. More recently, R. J. McIntyre has called attention to a calculation by Tager,⁴ which indicates that the noise power will in some cases increase faster than the signal power in the solid-state device, and has performed an independent calculation with the same conclusion.^{5, 6} Some experimental confirmation of this conclusion has been reported.⁷

McIntyre's results show that the variation of the diode mean-square noise current with multiplication depends on the ratio, α/β , of the electron and hole ionization coefficients. To obtain the limits of this variation, consider the expression⁷

$$I_n^2 = 2 q \Delta f [2 I_p(0) m^2(0) + 2 I_n(L) m^2(L) - I m^2(L) + 2 I \int_0^L \alpha m^2 dx + 2 q \int_0^L g m^2 dx] \quad (1)$$

The junction limits are 0 and L, $g(x)$ is the volume pair generation rate at the point X, $I_p(0)$ and $I_n(L)$ are the hole and electron currents being injected into the junction at $x = 0$ and $x = L$ respectively, I is the multiplied electron current, and $m(x)$ is a multiplication function defined by⁷

$$m(x) = \frac{\exp \left[\int_0^X (\alpha - \beta) dx' \right]}{1 - \int_0^L \beta \exp \left[\int_0^X (\alpha - \beta) dx' \right] dx} \quad (2)$$

Consider two limiting cases $\beta/\alpha = 1$ and $\beta/\alpha = 0$. There is no need to consider the range $1 \leq \beta/\alpha < \infty$, since the equations are symmetric in α and β , and this range for β/α therefore corresponds to the range 0 to 1 for α/β . Any asymmetry introduced by the boundary conditions can likewise be inverted by changing construction of the diode so that (for example) the n region is illuminated instead of the p region. In this discussion, it will be assumed that $\beta \leq \alpha$.

2.1.1.1 Case 1

Particularly simple results are obtained when $\alpha = \beta$. In this case m is not a function of x , and is

$$m = \left[1 - \int_0^L \alpha \, dx \right]^{-1} \quad (3)$$

Substituting this expression for m in Equation (1) yields

$$I_N^2 = 2 q \Delta f \left[2 I m^2 \left(1 - \frac{1}{m} \right) - I m^2 + 2 m I \right] \quad (4)$$

where I is the multiplied photocurrent, given by

$$I = m I_0 = m \left[I_p(0) + I_n(L) + \int_0^L q g \, dx \right] \quad (5)$$

It follows that

$$I_N^2 = 2 q \Delta f m^3 I_0 \quad (6)$$

The mean square noise current is proportional to the cube of the multiplication in this case.

2.1.1.2 Case 2

There is no other simple case where m is not a function of x . The integrals in the expression for the noise can, however, be performed

when $\beta/\alpha = 0$, and the only initiating current is electron injection. In this case, $g_0 = 0$, $I_p(0) = 0$, and

$$m(x) = \exp \left[\int_0^x \alpha \, dx' \right] . \quad (7)$$

If we define the overall multiplication of the injected electron current by M , then $M = m(L)$, $I = MI_n(L)$, and we obtain

$$I_N^2 = 2q\Delta f I_n(L) M^2 \left(2 - \frac{1}{M} \right) \quad (8)$$

For reasonably large multiplications, the mean square noise current is proportional to the square of the multiplication. This is the same relation obtained for a photomultiplier except for the 2 in the parenthesis. This factor occurs because both hole and electron current flow in a diode, and their fluctuations are independent. Hence the noise power is twice that observed in a photomultiplier.

We have thus shown that in the limiting cases $\beta/\alpha = 1$ and $\beta/\alpha = 0$, for large multiplications, the mean square noise current is proportional, respectively, to M^3 and M^2 .

Since it is desired that the noise power not increase more rapidly with multiplication than the signal power (which is proportional to M^2) it is necessary to work with as small a ratio of β/α as possible. This can be done in two ways: First by the choice of a diode with as small a ratio β/α as possible. Of those materials examined to date,⁸⁻¹¹ Si appears to have the smallest β/α ratio.

Second, examination of the variation of α and β with field^{8,9} shows that the ratio β/α (or α/β in the case of Ge) is smallest at low fields. It is therefore desirable to design the avalanching diode to operate at as low as a field as possible,¹² obtaining the necessary multiplication by lengthening the avalanche region.

Although use of the techniques described above will tend to minimize the excess noise in avalanche photodiodes, it can be expected that in any practical case, the mean square noise power from the diode will increase faster than the signal power. The usefulness of avalanche multiplication will therefore be determined by the thermal noise power due to the amplifier

following the diode. If the thermal noise power of this amplifier is larger than the diode noise power, multiplication can still produce an overall increase in signal-to-noise ratio. There will, however, be an optimum signal-to-noise ratio at some particular multiplication, and further multiplication will only degrade the signal-to-noise ratio. This may be seen in Figure 1 where signal and noise power and signal-to-noise ratio are sketched as functions of multiplication under the assumption that the noise power is proportional to $M^{2.5}$.

In summary, it is now believed that the noise in an avalanching photodiode will increase faster with multiplication than the signal; that this tendency may be minimized by the use of a material and a diode structure which keeps the ratio of the hole to the electron ionization coefficients as small as possible, and finally that sufficient avalanche multiplication to just overcome the thermal noise of the amplifier following the photodiode remains useful.

2.1.2 Frequency Response of Avalanching Photodiodes

One of the important questions connected with the use of avalanche multiplication to raise the signal and noise levels at the output of a photodiode is the effect of the multiplication process on the bandwidth of the device. The first determination of the bandwidth was reported by Lee and Batdorf.¹³ They applied the theory developed by Read¹⁴ for an avalanche microwave oscillator to the avalanching photodiode. The result indicated that the avalanche photodiode was subject to a gain-bandwidth product. The 3-db cutoff frequency was reported to be $\omega = 2/M\tau$, where M is the current multiplication, and τ is the transit time of a carrier across the entire junction region. The principle assumptions of the Read theory are that the ionization coefficients of electrons and holes are equal, and that the displacement current produced by the mobile charge in the avalanching portion of the junction may be neglected. (Avalanche multiplication is assumed to occur in only a small fraction of the junction space-charge region.)

Since this result represents a severe loss of bandwidth with multiplication, it was decided that it was important to make an attempt to improve the theory in the hope that operating conditions might be found which would yield a less severe bandwidth limitation.

A frequency response was therefore worked out exactly for a particularly simple case. The equations for carrier transport in an avalanching diode in which only electrons are capable of ionizing collisions, and in which

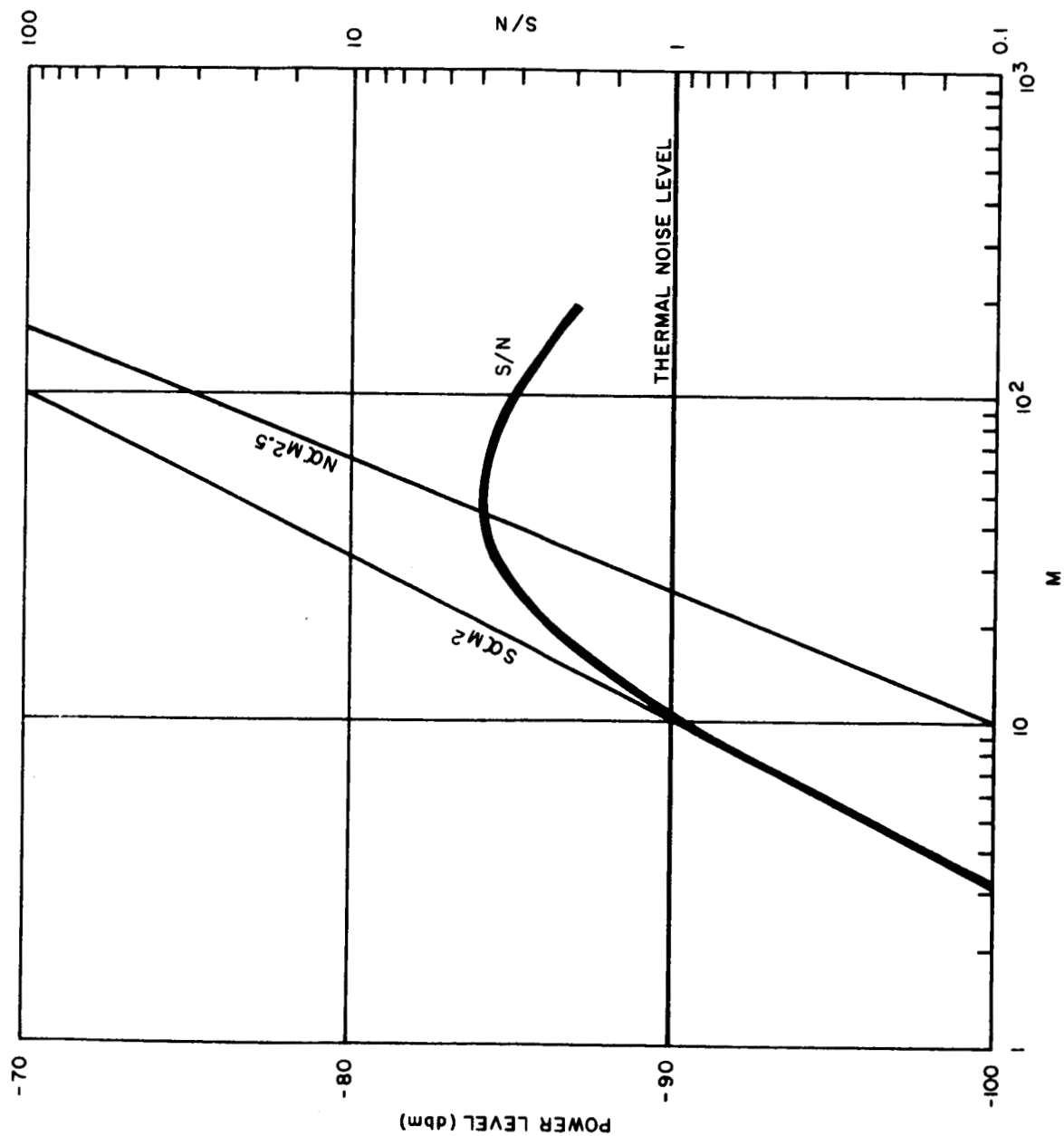


Figure 1. Signal-to-Noise Ratio Versus Multiplication

the multiplication is uniform throughout the junction are relatively simple mathematically. The frequency response obtained when electrons are injected into such a junction is essentially independent of current multiplication.¹⁵ In view of the strong contrast between this result and the result for the case of equal ionization coefficients for electrons and holes, a thorough analysis of the problem was undertaken. This analysis¹⁶ confirms that the behavior of the frequency response depends critically on the ratio α/β of the ionization coefficients for electrons to that for holes, and in particular yields the results discussed above for the two limiting cases: $\alpha/\beta = 0$, and $\alpha/\beta = 1$. For intermediate values of this ratio, the manner in which the bandwidth varies with multiplication is predicted only in a very general way. Since α and β are properties of the material from which the photodiode is constructed and hence can be selected only in a very limited sense, it is felt that further effort should be made to study the variation of frequency response with multiplication for arbitrary ratios of α to β . This is particularly important in view of the fact that the excess noise produced by the multiplication process (discussed above) is also dependent on the ratio α/β .

The differential equations governing the performance of a p-i-n avalanching photodiode when photogenerated electrons are injected have now been solved for arbitrary ratios of α to β . Unfortunately this solution was obtained after the termination of this contract, and frequency response curves have not been computed from it. It is included here for completeness.

We first obtain the ac components of the electron and hole currents in the junction. The differential equations to be solved are the coupled pair:⁵

$$\frac{dJ_n}{dx} + \left(\alpha - \frac{i\omega}{V_n} \right) J_n + \beta J_p = 0 \quad (9)$$

$$\frac{dJ_p}{dx} - \left(\beta - \frac{i\omega}{V_p} \right) J_p - \alpha J_n = 0 \quad (10)$$

These coupled equations may be separated. For example if we solve Equation (9) for J_p , differentiate, and substitute in Equation (10) we obtain a second order linear differential equation for J_n . An identical equation is

obtained for J_p . The general solutions to the equations are therefore of the form of "eigenvectors"

$$J_n = C_1 \exp(r_1 x) + C_2 \exp(r_2 x) \quad (11)$$

$$J_p = C_3 \exp(r_1 x) + C_4 \exp(r_2 x) \quad (12)$$

with the "eigenfrequencies" r_1 and r_2 .

Only two of the four constants in these equations can be independent since the original system is a pair of linear first order equations, each of which requires only one arbitrary constant. The two extra constants may be eliminated by substituting the solutions into the first order equations. Putting $a \equiv \left(\alpha - \frac{i\omega}{V_n} \right)$ and $b \equiv \left(\beta - \frac{i\omega}{V_p} \right)$ for simplicity, we have

$$\left[(r_1 + a) C_1 + \beta C_3 \right] \exp(r_1 x) + \left[(r_2 + a) C_2 + \beta C_4 \right] \exp(r_2 x) = 0 \quad (13)$$

$$\left[-a C_1 + (r_1 - b) C_3 \right] \exp(r_1 x) + \left[-a C_2 + (r_2 - b) C_4 \right] \exp(r_2 x) = 0 \quad (14)$$

Since x is the independent variable, these equations can vanish only if the coefficients of $\exp(r_1 x)$ and $\exp(r_2 x)$ vanish separately. We therefore have a pair of homogeneous equations in C_1 and C_3 , and a pair in C_2 and C_4 . Since the equations are homogeneous, nontrivial solutions exist only if the determinants of the coefficients vanish.

$$\begin{vmatrix} r_1 + a & \beta \\ -a & r_1 - b \end{vmatrix} = 0 \quad (15)$$

$$\begin{vmatrix} r_2 + a & \beta \\ -a & r_2 - b \end{vmatrix} = 0 \quad (16)$$

These are the "secular" equations of the system, and yield for the eigen-frequencies

$$r_{1,2} = -\frac{(a-b)}{2} \pm \left[\left(\frac{a-b}{2} \right)^2 + (ab - a\beta) \right]^{1/2} \quad (17)$$

If this equation is satisfied, we may write for the ratios C_1/C_3 and C_2/C_4 ,

$$\frac{C_1}{C_3} = -\frac{\beta}{(r_1 + a)} = \frac{(r_1 - b)}{a} \quad (18)$$

$$\frac{C_2}{C_4} = -\frac{\beta}{(r_2 + a)} = \frac{(r_2 - b)}{a} \quad (19)$$

The eigenvectors are then

$$J_n = C_1 d^{r_1 x} + C_2 e^{r_2 x} \quad (20)$$

$$J_p = -(1/\beta) \left[(r_1 + a) C_1 e^{r_1 x} + (r_2 + a) C_2 e^{r_2 x} \right] \quad (21)$$

The remaining two arbitrary constants may be removed by application of the boundary conditions. If a photogenerated electron current J_0 is injected at $x = L$, then the boundary conditions are

$$J_n(L) = J_0, \quad J_p(0) = 0 \quad (22)$$

and the currents are

$$J_n = J_0 \frac{\left[(r_2 + a) e^{r_1 x} - (r_1 + a) e^{r_2 x} \right]}{\left[(r_2 + a) e^{r_1 L} - (r_1 + a) e^{r_2 L} \right]} \quad (23)$$

$$J_p = - \frac{aJ_o \left[e^{r_1 x} - e^{r_2 x} \right]}{\left[(r_2 + a) e^{r_1 L} - (r_1 + a) e^{r_2 L} \right]} \quad (24)$$

The short-circuit ac current in the load is given by

$$J = \frac{1}{L} \int_0^L (J_n + J_p) dx$$

$$= \frac{J_o}{L} \frac{\left[(r_2 + a - a) r_2 (e^{r_1 L} - 1) - (r_1 + a - a) (e^{r_2 L} - 1) \right]}{r_1 r_2 \left[(r_1 + a) e^{r_1 L} - (r_1 + a) e^{r_2 L} \right]} \quad (25)$$

To obtain the frequency response, the current may be normalized by dividing by the multiplied dc current, i.e.,

$$F(\omega) = J/MJ_o$$

where

$$M = J_o \frac{(\alpha - \beta) \exp [(\alpha - \beta) L]}{\alpha - \beta \exp [(\alpha - \beta) L]}$$

For the limits $\alpha/\beta = 0$ and $\alpha/\beta = 1$, this function reduces to the frequency response functions already obtained.

2.2 EXPERIMENTAL WORK

2.2.1 Material Studies

The use of X-ray "rocking curves" was investigated as a possible technique for obtaining information on the crystalline perfection of the InAs from which the photodiodes were to be made.^{17, 18} The rocking curve

is a measure of the intensity of the X-rays reflected from the surface of the InAs wafer, as a function of angle, as the wafer is rotated slightly in the vicinity of the Bragg angle. The angular width of the rocking curve can be correlated with the size of a laue spot. The X-rays incident on the sample must be as parallel as possible, and in practice the source consisted of 1.54 \AA CuK α radiation reflected from a second InAs crystal oriented in the same way as the sample under investigation.

It was found that the surface damage caused by mechanical polishing could be easily detected in this way. The width of the rocking curves for etched material was 30 inches; for polished material 60 inches. It was also found that the diffusion used to make the p-n junctions tended to double the width of the rocking curve, although the effect of the diffusion did not appear to be uniform over the surface of the wafer. There are further comments on this diffusion below.

In an effort to obtain a correlation between crystalline perfection and diode quality, six diodes were made from a wafer of InAs purposely chosen to contain a wide variation in dislocation-count density. X-ray rocking curves and Schutz photographs as well as etch-pit counts showed an area of the wafer with a heavy density of lines of dislocations which terminated on what appeared to be a slip plane parallel to the growth axis of the crystal. The zero-bias resistance, the dark-current density and the avalanche multiplication of these diodes was measured. The dark-current densities of the diodes made from the heavily dislocated material were materially higher than the dark-current densities of the remaining diodes. The other two parameters showed no clear correlation with dislocation count.

It had become clear during the course of this work that the crystalline perfection of bulk InAs is not as good as that of bulk GaAs, and preliminary work had been initiated to obtain epitaxial films of InAs grown on GaAs substrates. This technique should produce InAs of as good quality as the substrate. This work, however, was not emphasized because of the lack of correlation of the quality of the starting material with current multiplication observed. This lack of correlation seemed to indicate that the diode fabrication techniques were limiting the multiplication. In particular it was decided to investigate the possibility of obtaining a guard-ring structure in InAs.

2.2.2 Guard-Ring Studies

An important step in the attainment of uniformity and control over breakdown Si and Ge has been the introduction of guard rings to

reduce the field at the intersection of the junction with the surface.^{19, 20} An investigation of the possibility of obtaining a guard-ring structure in InAs was therefore begun. The investigation was directed toward obtaining a weak deep ring-shaped Mn diffusion upon which could be superimposed a strong central Cd diffusion. The use of Mn for the guard-ring was suggested by previous work in this laboratory which indicated that an Mn diffusion is somewhat slower and therefore easier to control than the Cd diffusion normally used to make InAs photodiodes. Published diffusion studies for impurities in InAs^{21, 22} do not include data on Mn.

The Mn diffusion was accomplished by evaporating approximately $100 \mu\text{gm}/\text{cm}^2$ of Mn on an etched InAs wafer, and heating in an oven at $750\text{-}760^\circ\text{C}$. Temperatures in this range produce a junction depth of approximately 2 microns in 5 minutes in 10^{17} cm^{-3} n-type InAs. After the Mn diffusion, the excess Mn on the surface was removed, and the wafer was etched until n-type was present everywhere except in a ring-shaped area. A 1-minute open-tube Cd diffusion was then performed, during which the Mn ring was driven somewhat deeper, and a mesa was etched. The diode structure is sketched in Figure 2.

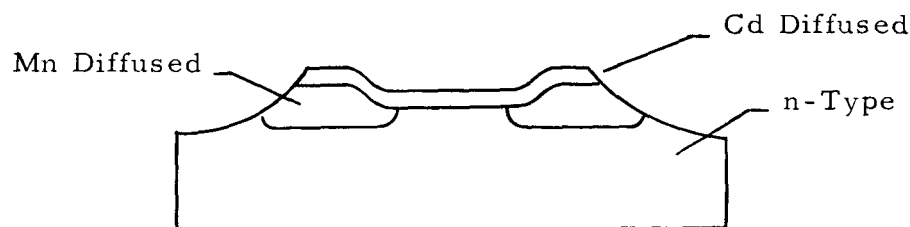


Figure 2. Sketch of Proposed InAs Guard-Ring Diode

These diodes showed a high leakage current, and thermal probing indicated that the Mn-doped region was more strongly p-type than the Cd-doped region. This is opposite to the effect desired.

A possible cause of this difficulty is the difference between the types of source used in the Mn and Cd diffusions. Because of the low vapor pressure of Mn, an evaporated layer must be used as a source in this case, while in the case of Cd, a vapor source may be used. This difference may result in a higher surface concentration for the Mn diffusion. A number of methods of remedying the difficulty suggested themselves. Since the Cd vapor diffusion produces a less-heavily doped p layer than the Mn diffusion, consideration was given to reversing the

roles of the two diffusions; using the Cd diffusion to produce the guard ring, and the Mn diffusion to produce the photodiode. Consideration was also given to a reduction of the Mn concentration by diffusing through an SiO_2 layer deposited on the InAs surface. Alternately, it may be noted that as the depth of a diffusion is increased, the concentration gradient at the diffusion front decreases. Therefore a lower Mn concentration might be obtained by performing a deep diffusion, and then etching most of the diffused layer away.

The first two of these remedies were pursued. Whether it is desirable to use the Cd diffusion for the guard ring and the Mn diffusion for the photodiode depends on whether or not Mn-diffused photodiodes can be obtained which are of a quality at least as good as the Cd-diffused photodiodes presently being made. A number of Cd and Mn photodiodes were therefore prepared from the same starting material. It was found that the zero-bias resistance and leakage currents of the Mn-diffused diodes were poorer than those of the Cd-diffused diodes by factors of 3 and 8 respectively.

The use of an SiO_2 coating, deposited on the InAs thermal decomposition of silane, to reduce the concentration of the Mn diffusant, was next investigated.²³ It was found that when the SiO_2 was deposited at a temperature in excess of 500°C , very large numbers of etch pits developed in the InAs surface. This problem can be avoided during the SiO_2 formation, but not during the diffusions, for which temperatures in excess of 700°C are required.

Work on guard-ring structures was discontinued at this point in order to allow time for the production and testing of the sample diodes required by this contract. The development of a guard-ring structure to improve the uniformity and reproducibility of the breakdown characteristics of InAs (and of III-V compound diodes in general) remains, however, an important subject for future work. A recent unpublished report²⁴ contains data on a technique for controlling the p-type diffusants used in III-V compounds which may yield better results than those reported above. The technique is based on Raoult's law, which states that the vapor pressure of one component of a mixture over the mixture is proportional to its concentration in the mixture. For example, at a fixed temperature, the vapor pressure of Cd over an alloy of Cd and Ga is proportional to the percentage of Cd in the alloy. In addition, since Ga has a very much lower vapor pressure than Cd, its effects in the diffusion may be ignored. In a closed-tube Cd diffusion, the vapor pressure of the diffusant can therefore be adjusted independently of the temperature

by adjusting the diffusant concentration in the source alloy. This technique permits use of a small diffusion tube and a single-temperature diffusion oven, without loss of control over the diffusant vapor pressure.

Previous efforts to use Cd and Zn vapor diffusions in III-V compounds in a single-temperature-zone oven required that the mass of diffusant inserted in the diffusion tube be carefully limited in order to avoid surface alloying. The result was a high initial vapor pressure (which made it difficult to produce low surface concentrations) and a subsequently decreasing vapor pressure (which made it difficult to produce deep junctions). It was these difficulties with closed-tube diffusions which prompted the development of the open-tube Cd diffusion for InAs which has been in use in this laboratory.

Kendall's report²⁴ on the use of alloy diffusion sources included no new work on InAs. He reports, however, the ability to control Zn surface concentrations in InSb diodes over at least two orders of magnitudes. If this behavior can be obtained in InAs as well, it appears possible to adapt this diffusion technique to the production of a guard-ring diode using, for example, two separate Cd diffusions. The first, to produce the guard ring, would employ a low vapor pressure Cd source. The second, with a high vapor pressure, would produce the central photosensitive area in the normal way.

In summary, it is believed that enhancement of the avalanche multiplication of the photocurrent in InAs can be obtained by producing more uniform breakdown characteristics in the diodes. An important step in obtaining this uniformity is the development of a guard-ring structure. Attempts to obtain a guard-ring structure in InAs have been unsuccessful. Improved control over Cd and Zn diffusion using an alloy source have been demonstrated in InSb, and it is suggested that the application of this technique may lead to the desired result in InAs.

2.2.3 Diode Fabrication and Testing

2.2.3.1 Fabrication

The fabrication and testing procedures used on the InAs photo-diodes being made at the conclusion of this contract are described here. The primary emphasis of these procedures was on current multiplication obtainable, which was of the order of 10.

On the basis of current multiplication, diodes made from material with a doping density of approximately $1 \times 10^{17} \text{ cm}^{-3}$ were found most satisfactory. The diodes reported were made from n-type tin-doped InAs with a doping density between 8.5 and $9.5 \times 10^{16} \text{ cm}^{-3}$, and a mobility of $21,000 \text{ cm}^2 \text{ v}^{-1} \text{ sec}^{-1}$. To prepare the diodes, a wafer of this material is first etched in a solution of 4 parts of 50 percent HF, 12 parts of 70 percent HNO_3 , and 18 parts of H_2O . The wafer is then placed, "B" side up, on a quartz slide and covered with a quartz cap of about 3 cm^3 volume. About 10 milligrams of Cd is placed in a small side tube inside this cap. The quartz slide is then pushed into an oven at 810°C , through which forming gas is flowing, diffused for 1 minute, and cooled quickly. The depth of the junction produced by this open-tube diffusion is approximately 3 microns.

After removal from the oven, drops of Kel-F 200 (Minnesota Mining and Manufacturing Co.) approximately 10 mils in diameter are placed on the "B" side of the wafer. The wafer is then given several 5-second etches followed by water rinses, leaving a diffused p layer only under the wax. The wax is then removed from the mesa area by cooling the wafer to 77°K and mechanically peeling it off. Diode dice about 40 mils by 40 mils, each containing a sensitive mesa, are then scribed and cleaved from the wafer. Each die is soldered to a mount with In and, after a 1-second clean-up etch, a 1-mil Pt wire is soldered to the mesa, also with In.

2.2.3.2 Testing

The reverse-bias current-voltage characteristics of the InAs photodiodes were measured at low frequency, and multiplication data were obtained both at low frequency and at 125 MHz. The high-frequency data was obtained by measurement of the amplitude of the beat-frequency signal from the diode, as a function of bias, when He-Ne laser light containing several axial modes was incident on the diode. The current multiplication data is obtained from these high-frequency measurements by assuming that the signal obtained when the bias (in volts) is less than the InAs band gap (in eV) is not multiplied. The signal obtained at larger reverse biases is then compared with this unmultiplied signal. The multiplication data at low frequency is obtained by comparing the difference between the diode reverse current with and without light incident to the light current measured at zero bias.

The reverse bias characteristics and the multiplication data are shown in Figures 3 through 18. None of the diodes show a true saturation in the reverse direction. Generation and recombination in the junction can

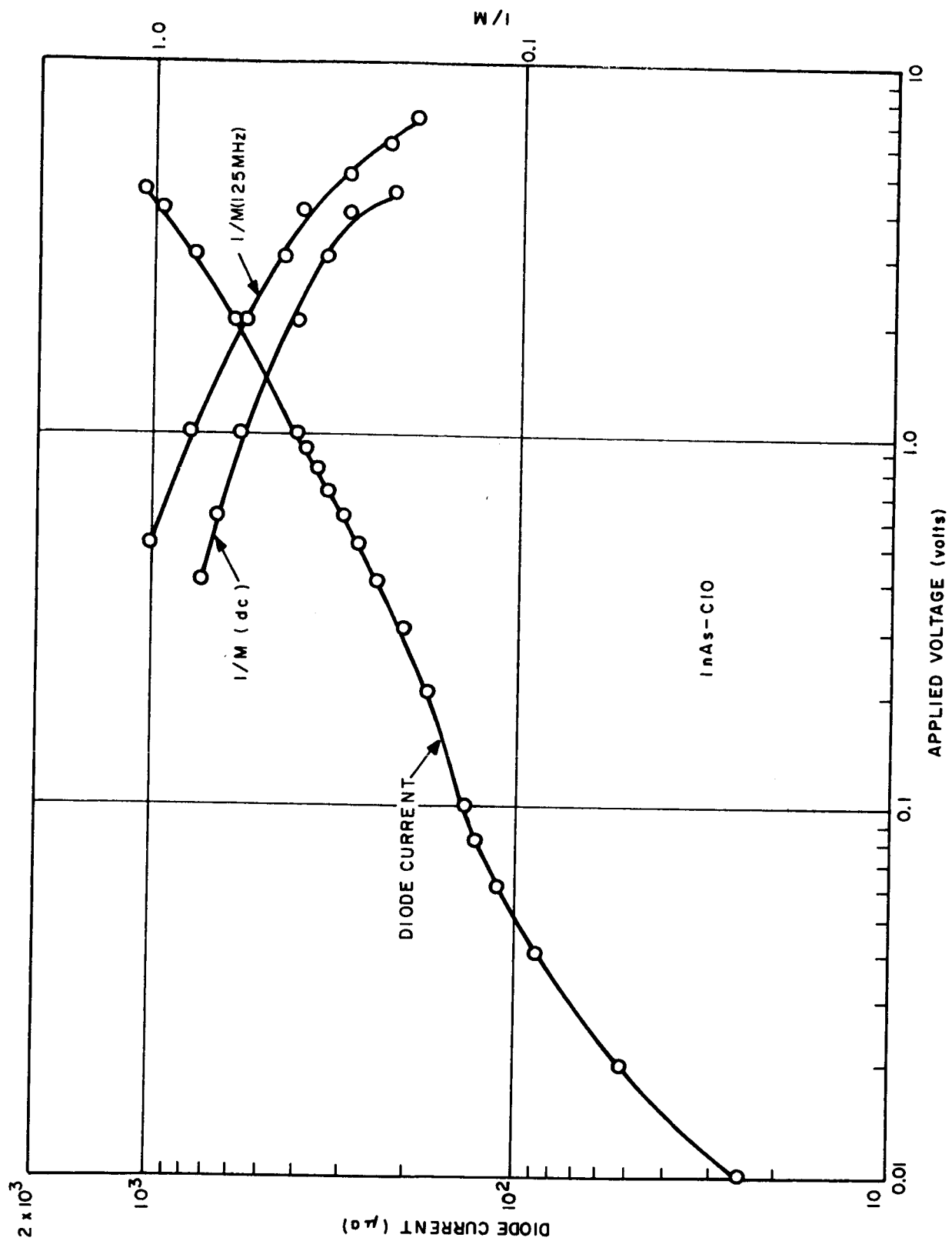


Figure 3. Reverse Bias Current — Voltage and Current Multiplication Characteristics for InAs-C10

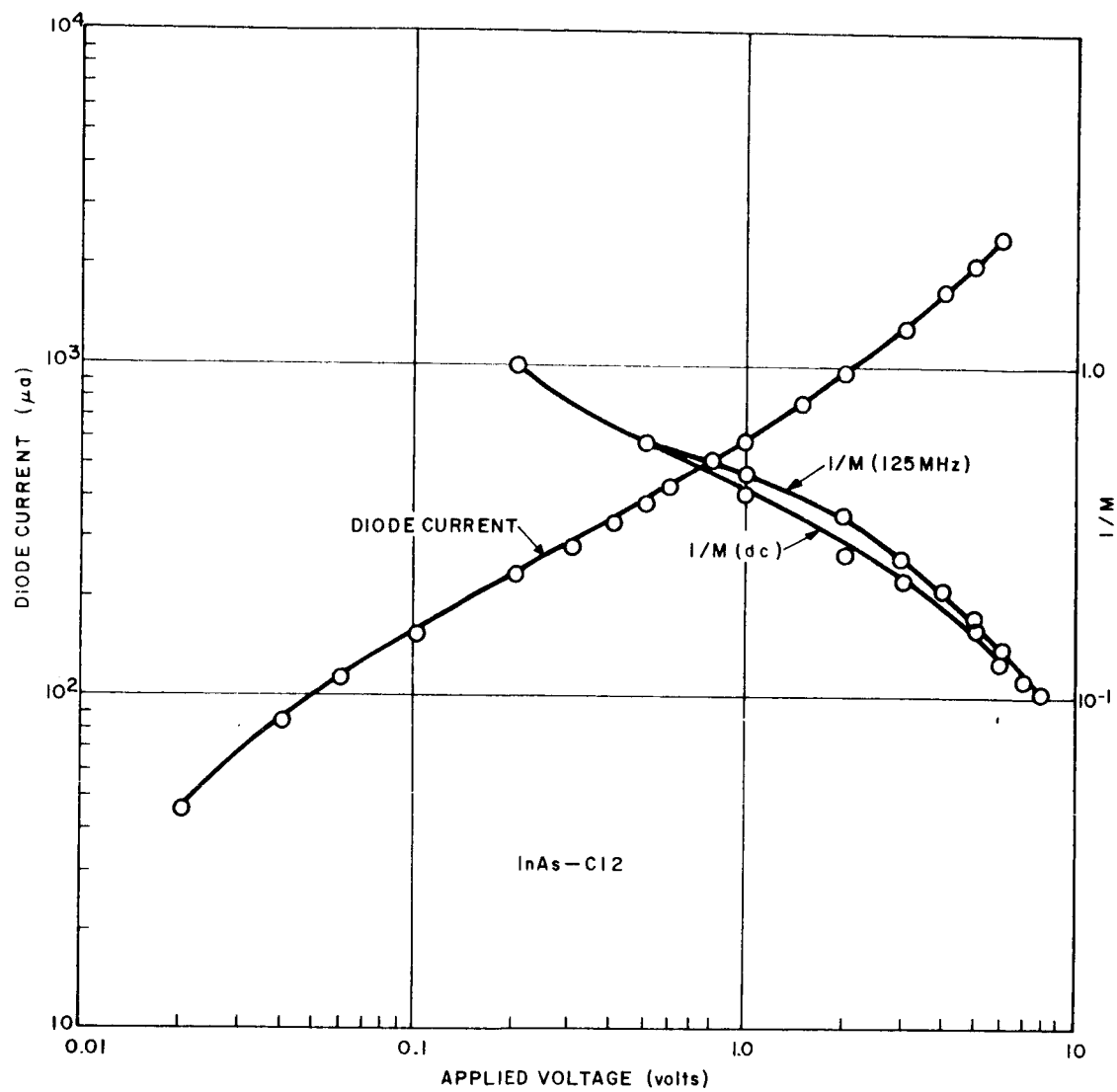


Figure 4. Reverse Bias Current — Voltage and Current Multiplication Characteristics for InAs-C12

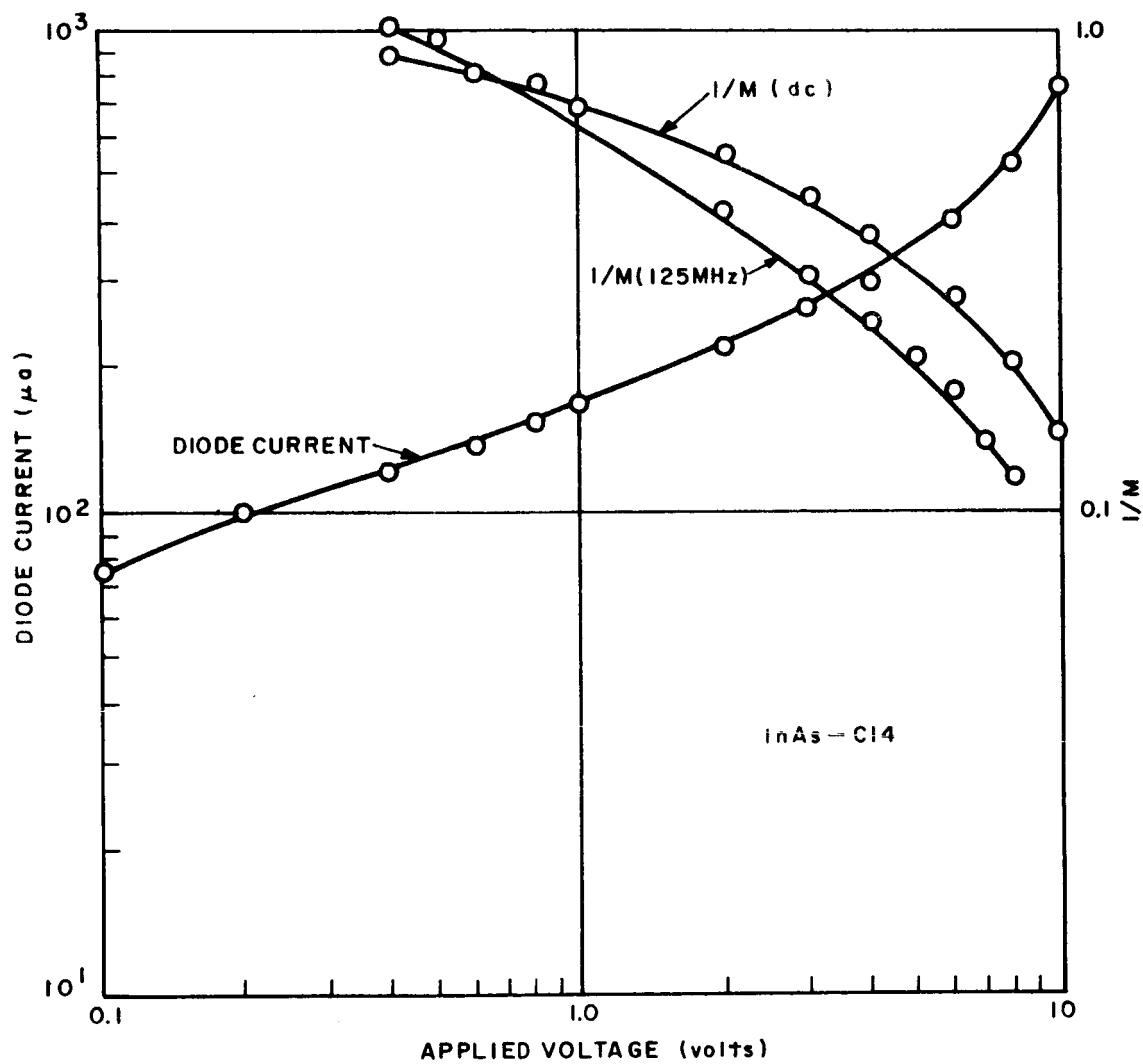


Figure 5. Reverse Bias Current — Voltage and Current Multiplication Characteristics for InAs-C14

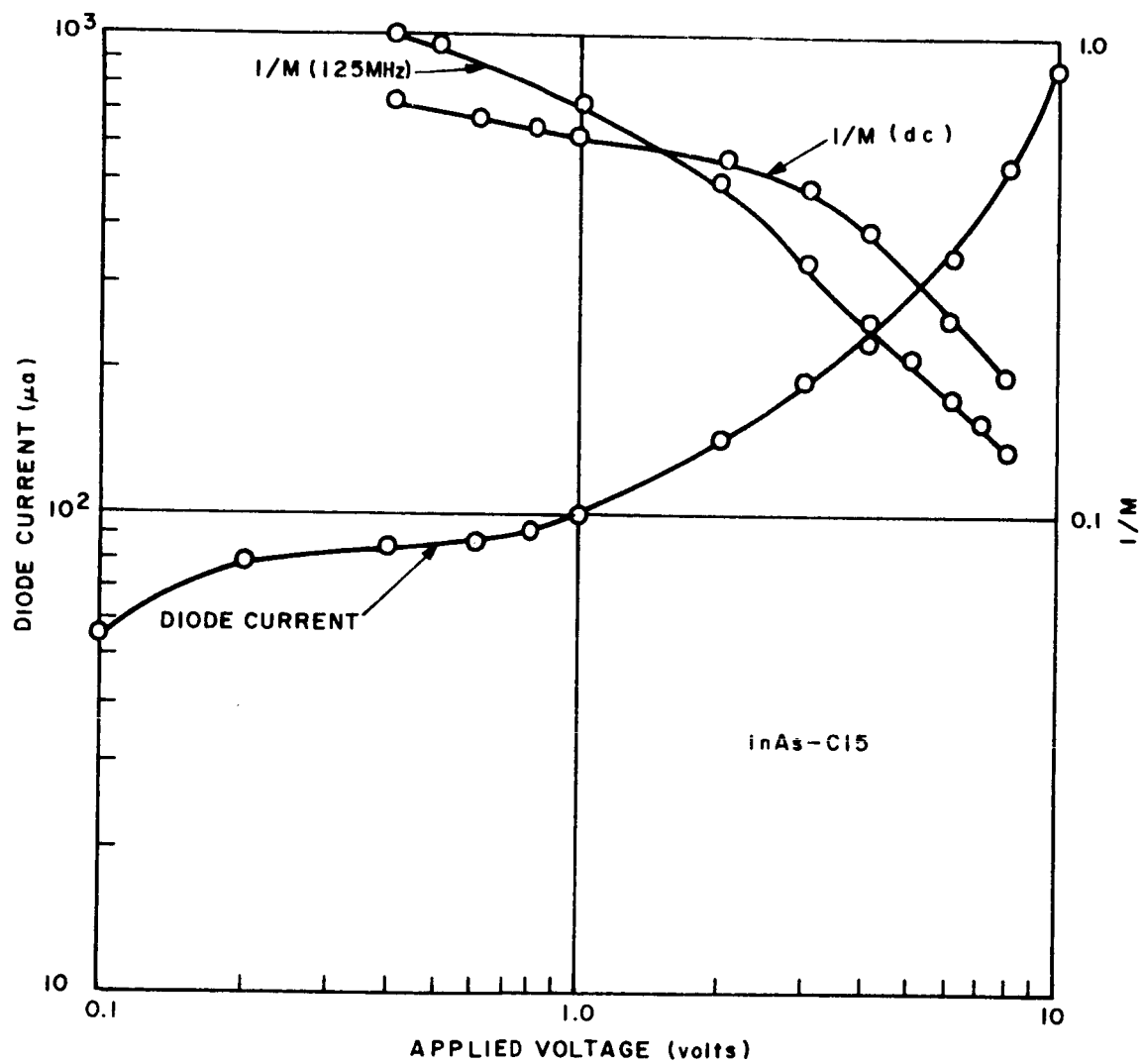


Figure 6. Reverse Bias Current — Voltage and Current Multiplication Characteristics for InAs-C15

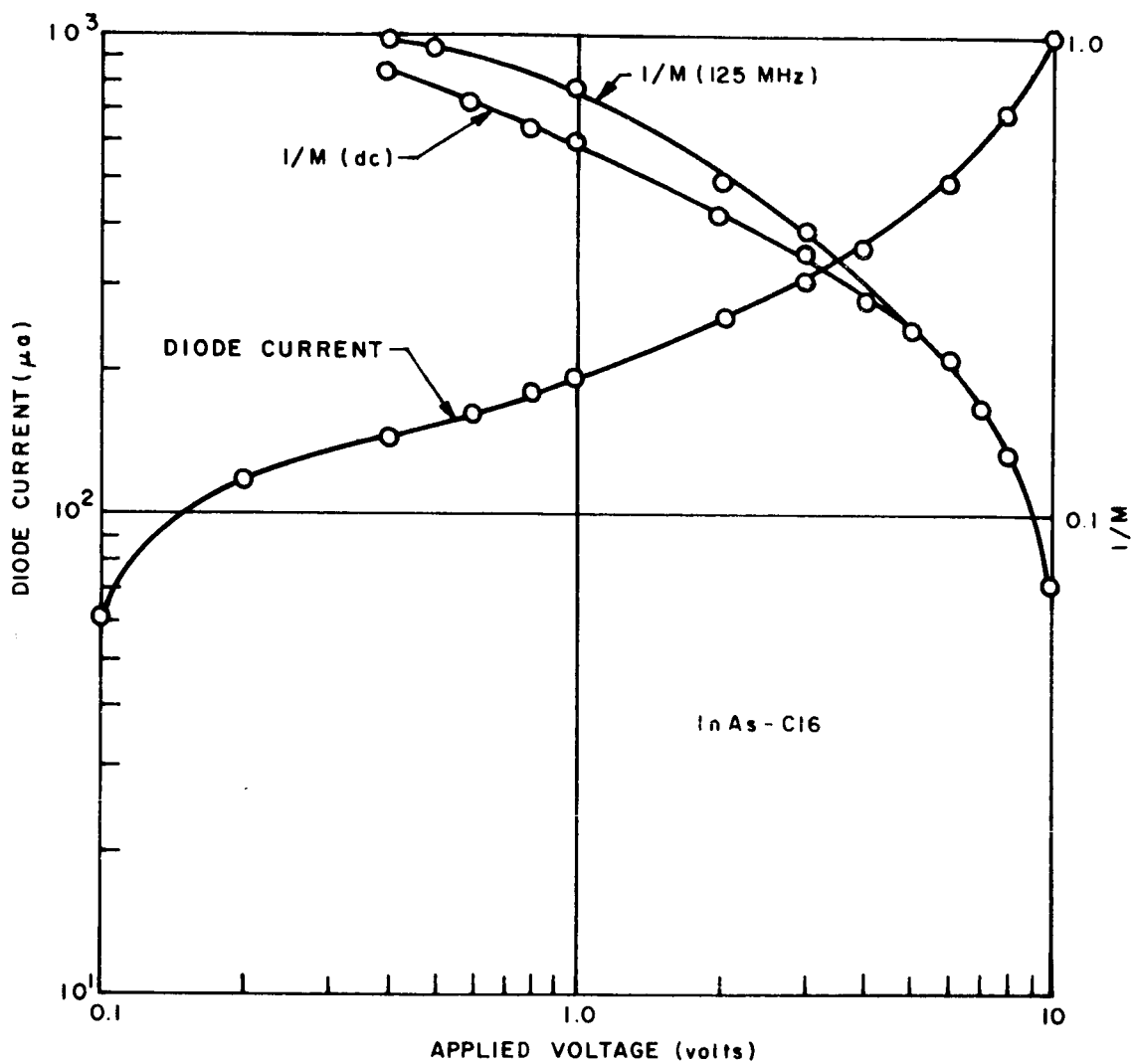


Figure 7. Reverse Bias Current — Voltage and Current Multiplication Characteristics for InAs-C16

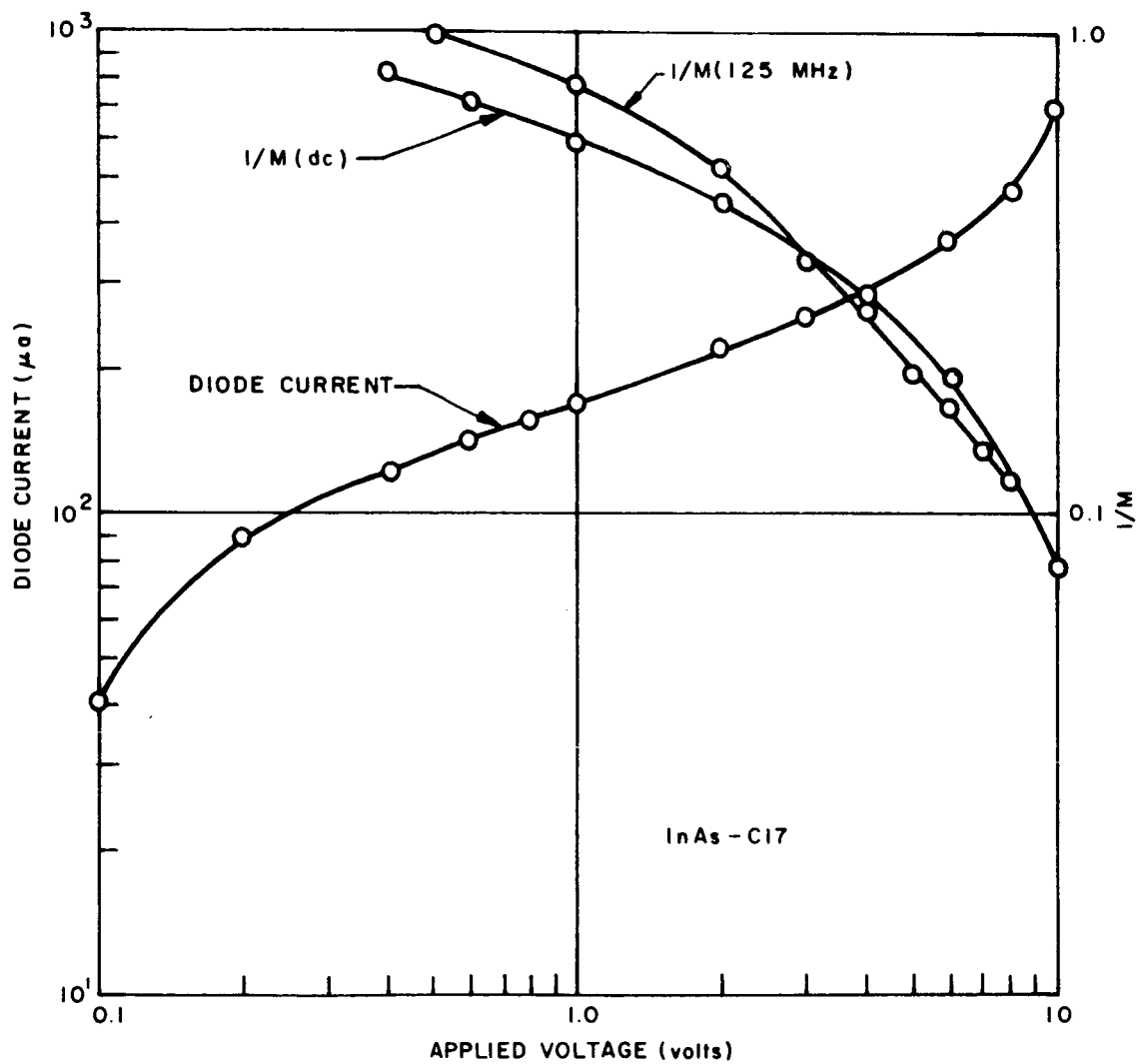


Figure 8. Reverse Bias Current — Voltage and Current Multiplication Characteristics for InAs-C17

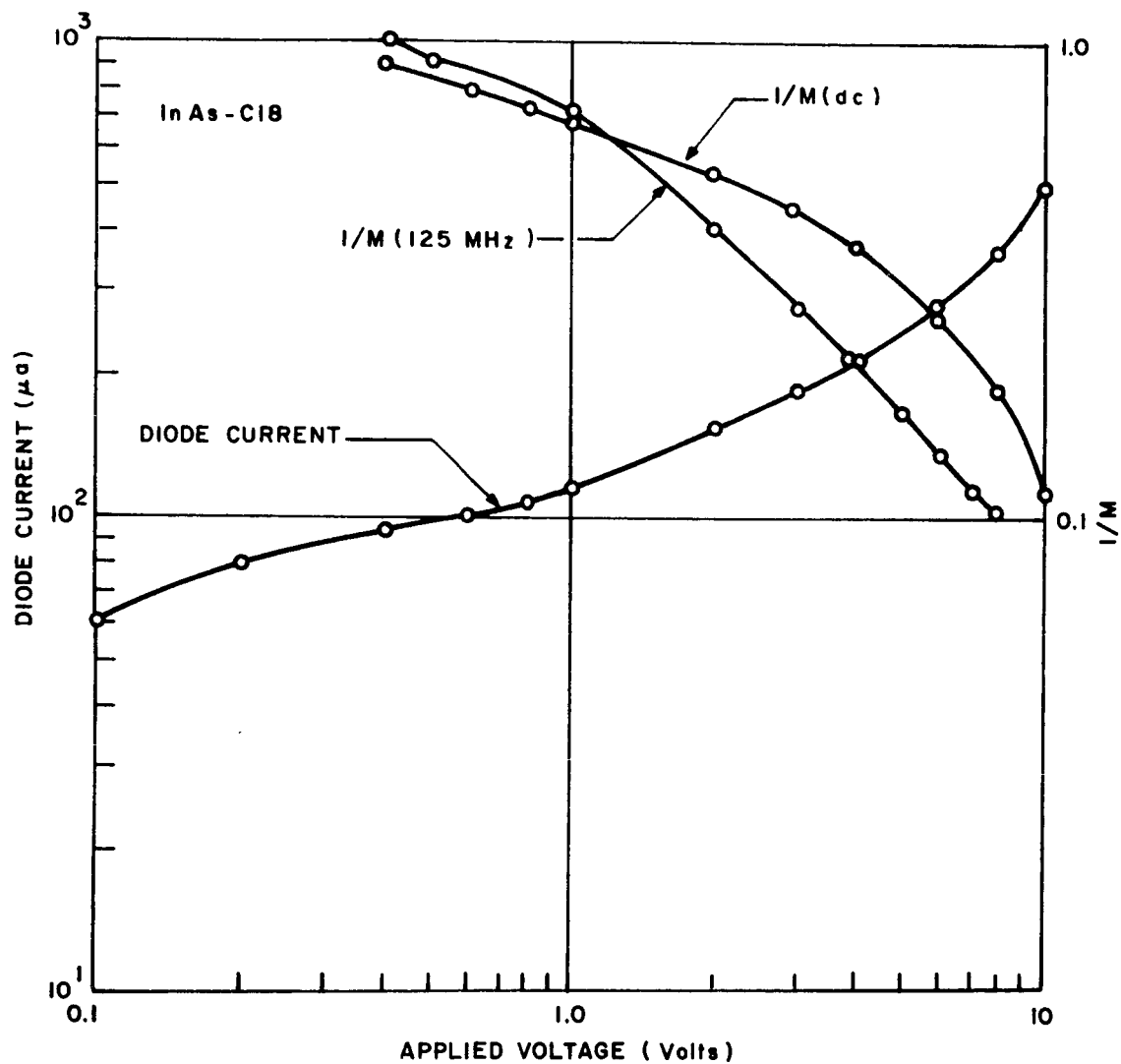


Figure 9. Reverse Bias Current — Voltage and Current Multiplication Characteristics for InAs-C18

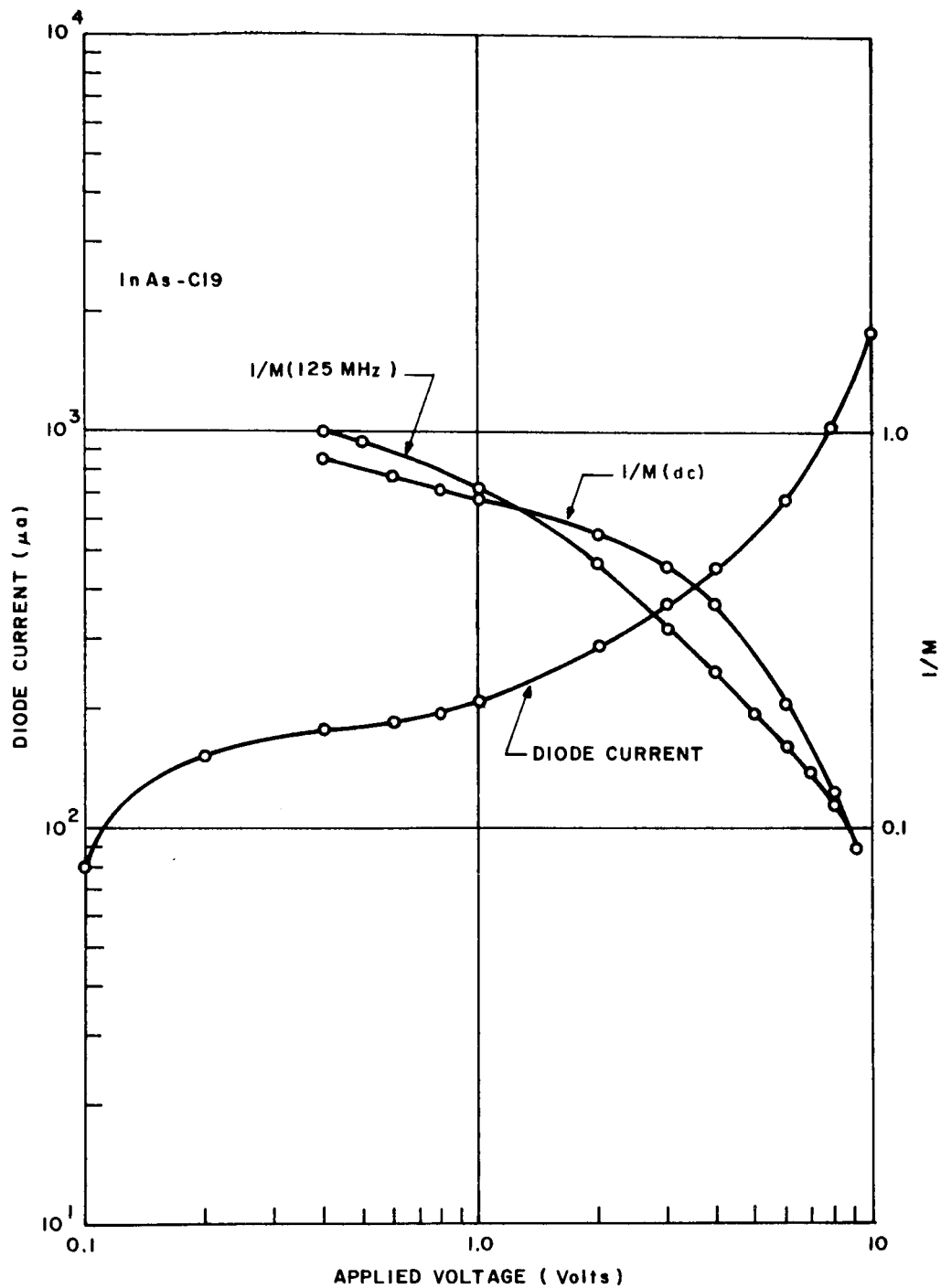


Figure 10. Reverse Bias Current — Voltage and Current Multiplication Characteristics for InAs-C19

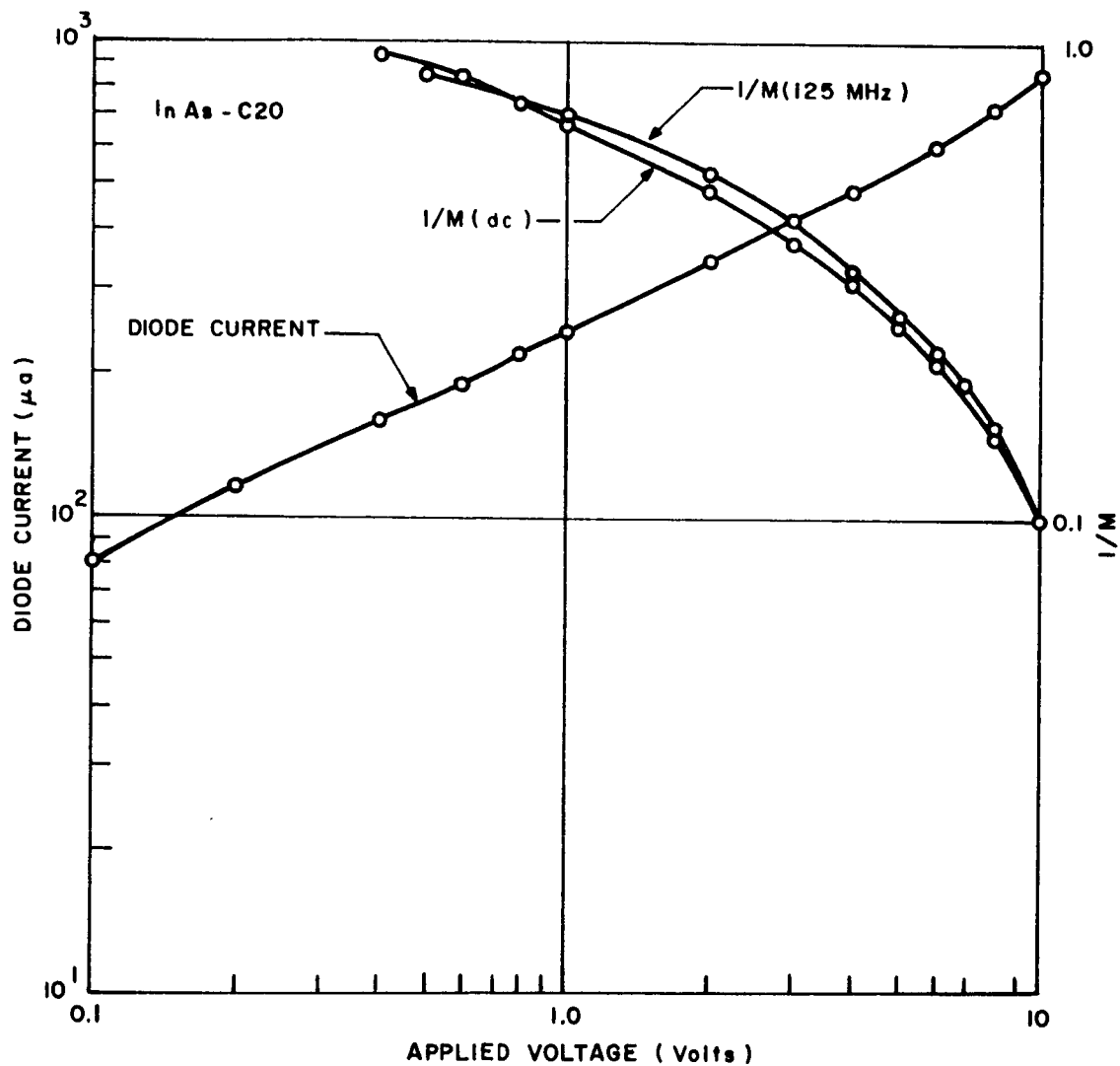


Figure 11. Reverse Bias Current — Voltage and Current Multiplication Characteristics for InAs-C20

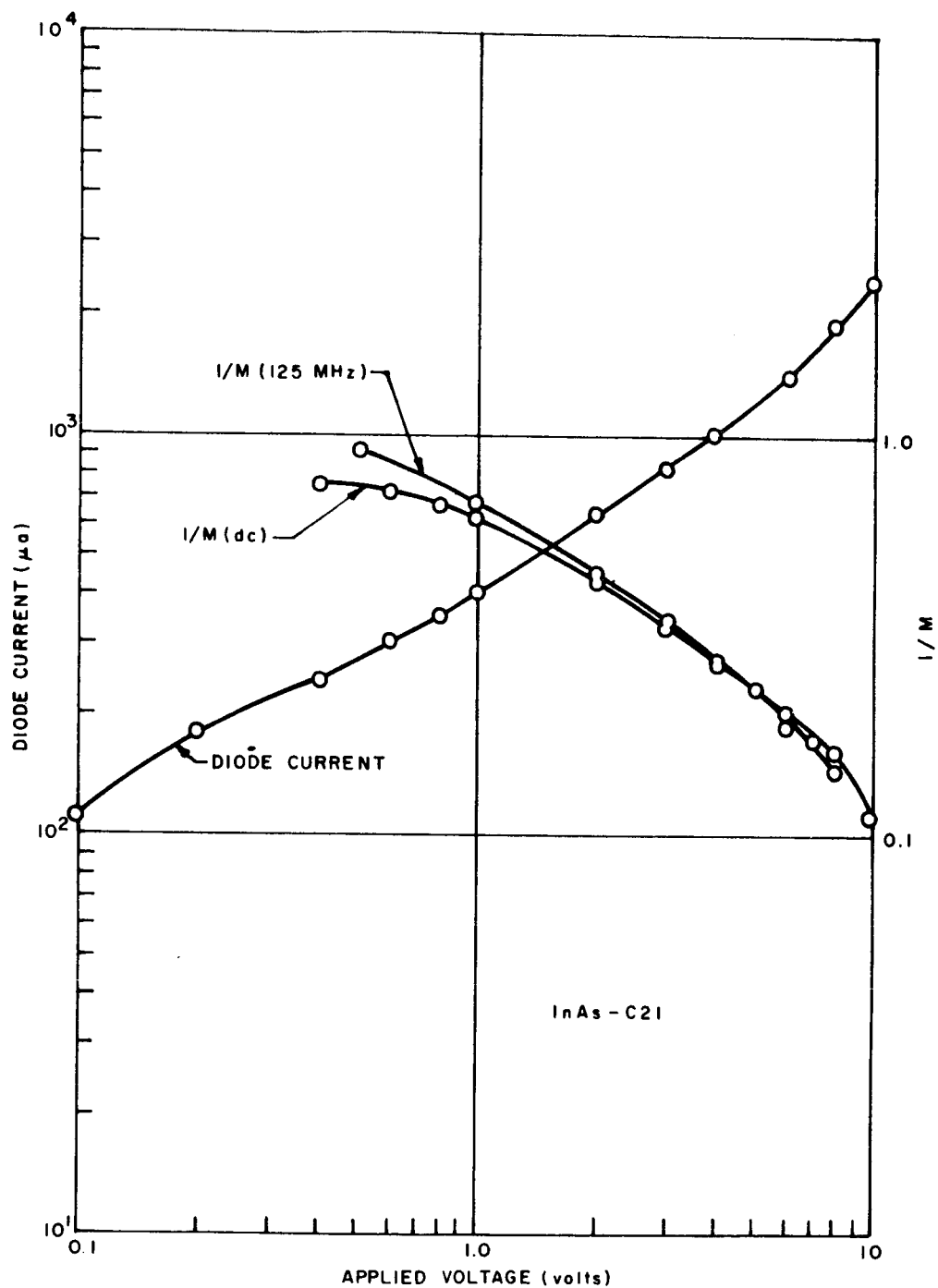


Figure 12. Reverse Bias Current — Voltage and Current Multiplication Characteristics for InAs-C21

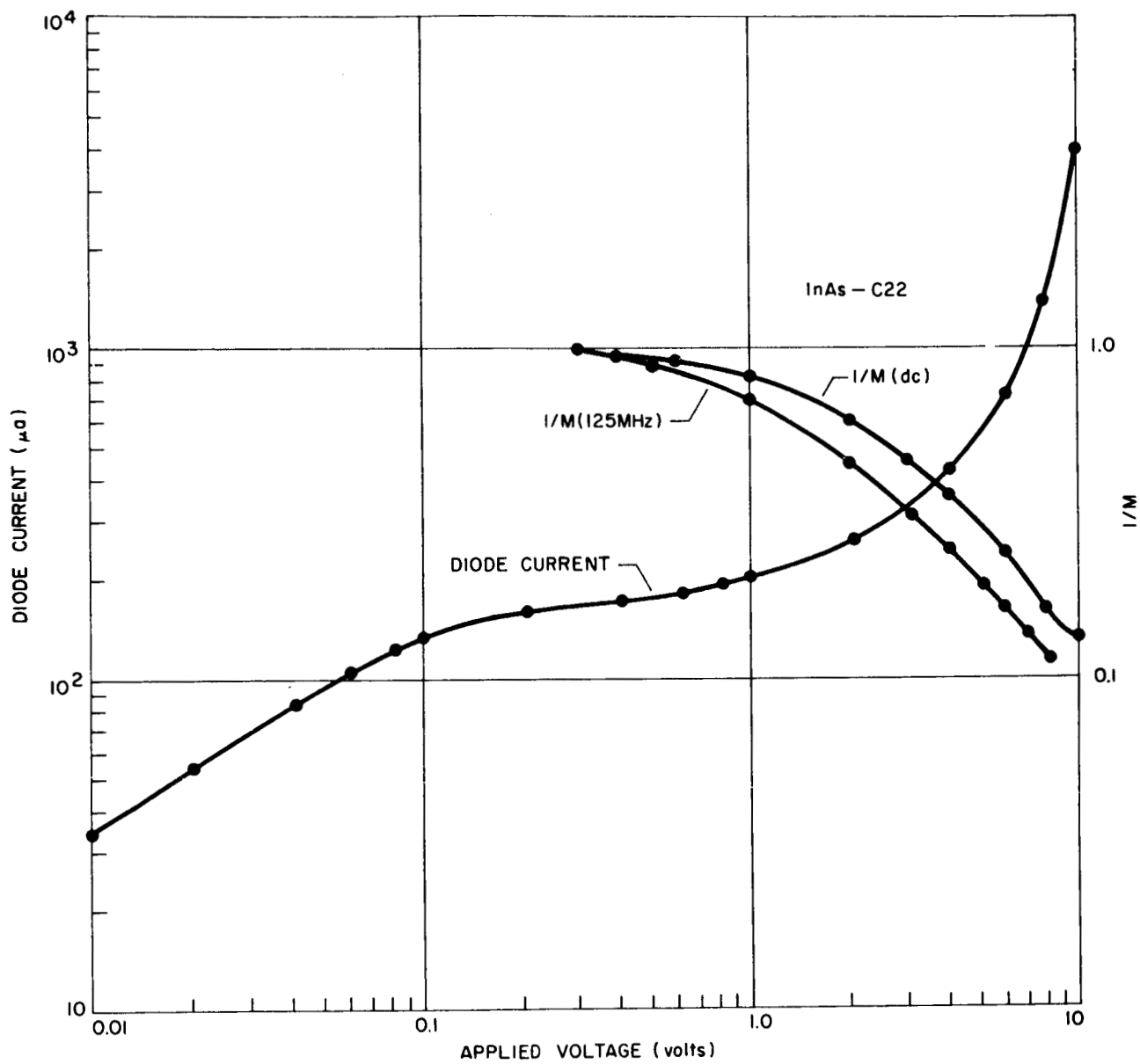


Figure 13. Reverse Bias Current - Voltage and Current Multiplication Characteristics for InAs-C22

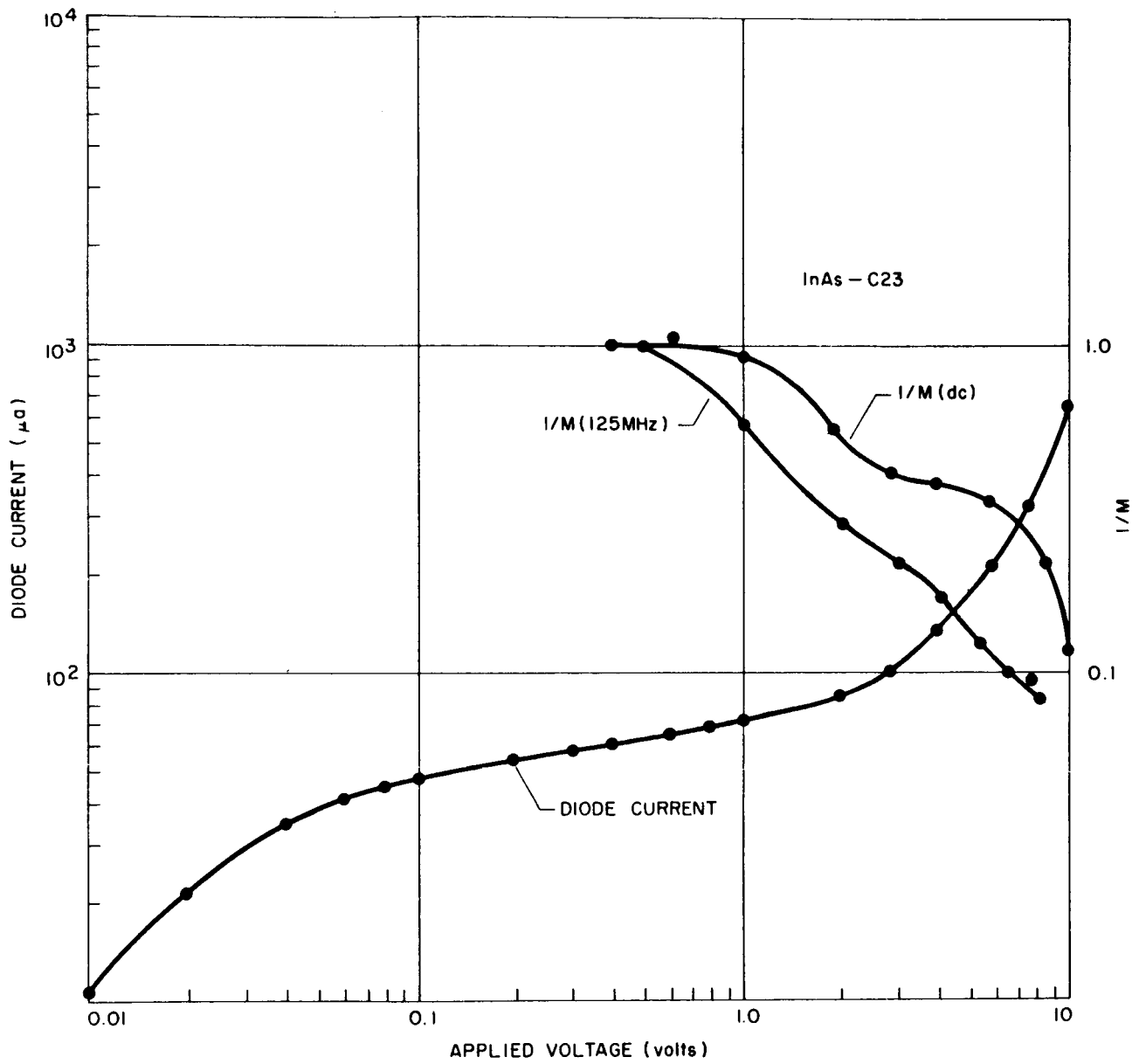


Figure 14. Reverse Bias Current-Voltage and Current Multiplication Characteristics for InAs-C23

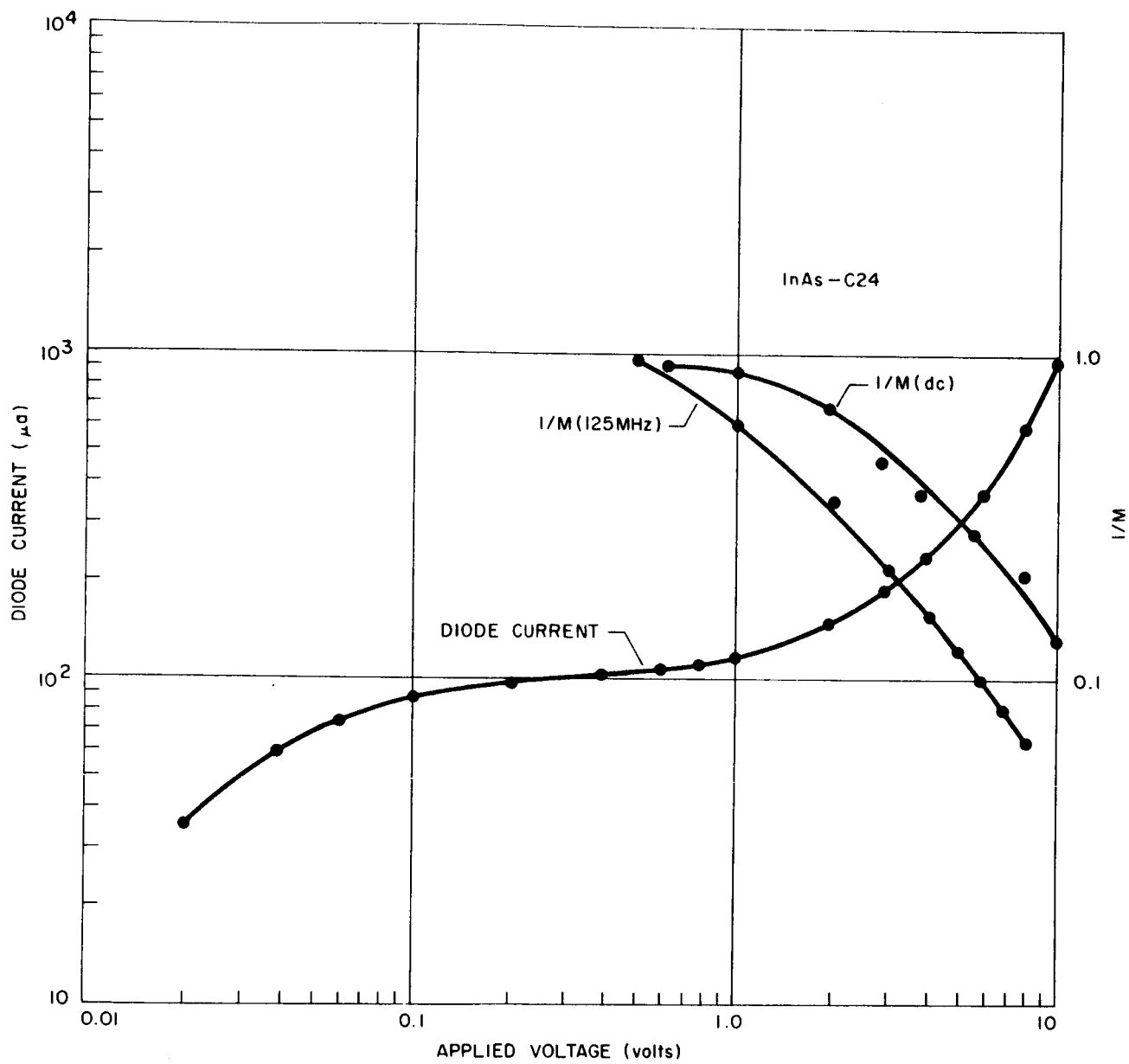


Figure 15. Reverse Bias Current-Voltage and Current Multiplication Characteristics for InAs-C24

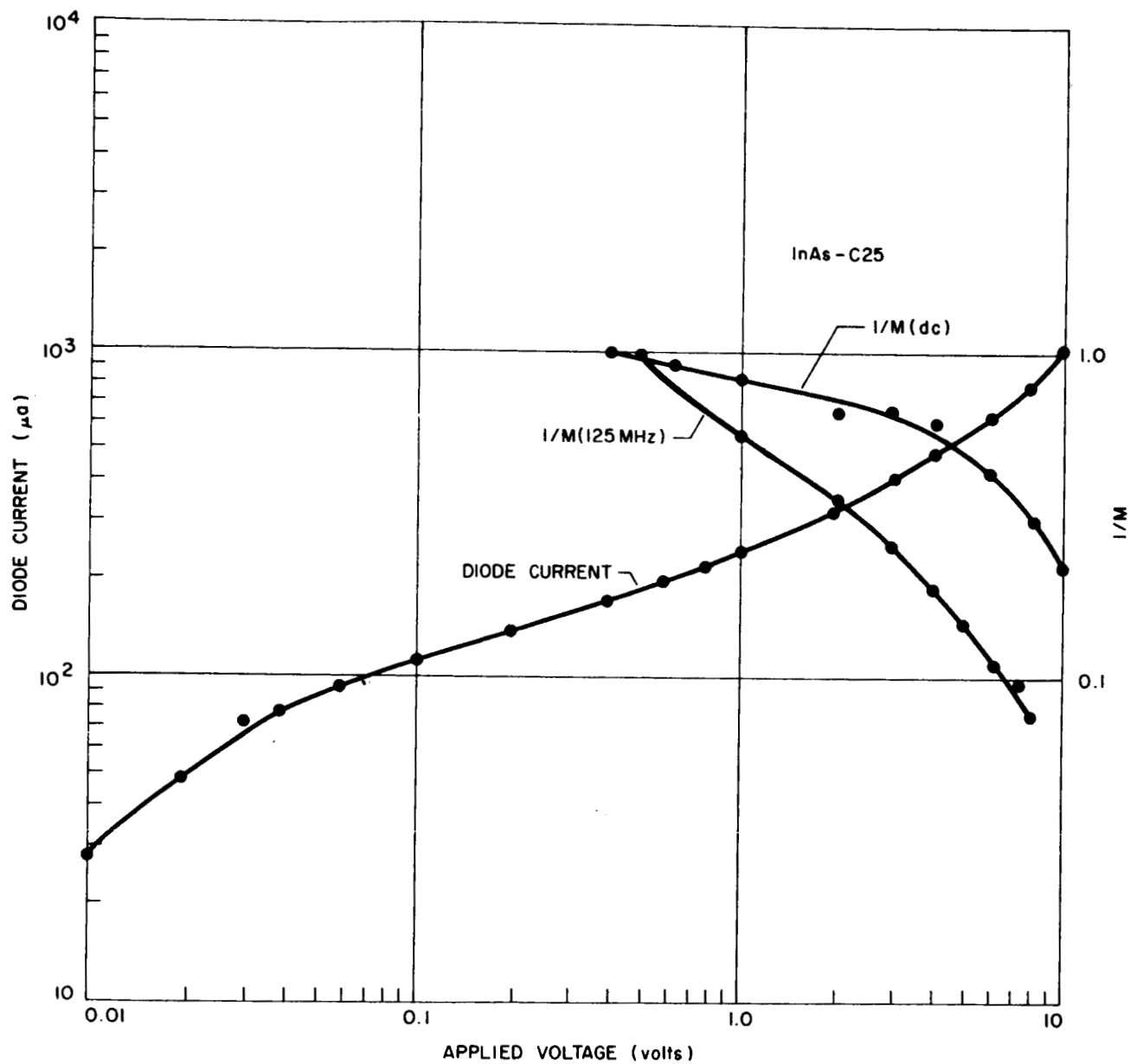


Figure 16. Reverse Bias Current-Voltage and Current Multiplication Characteristics for InAs-C25

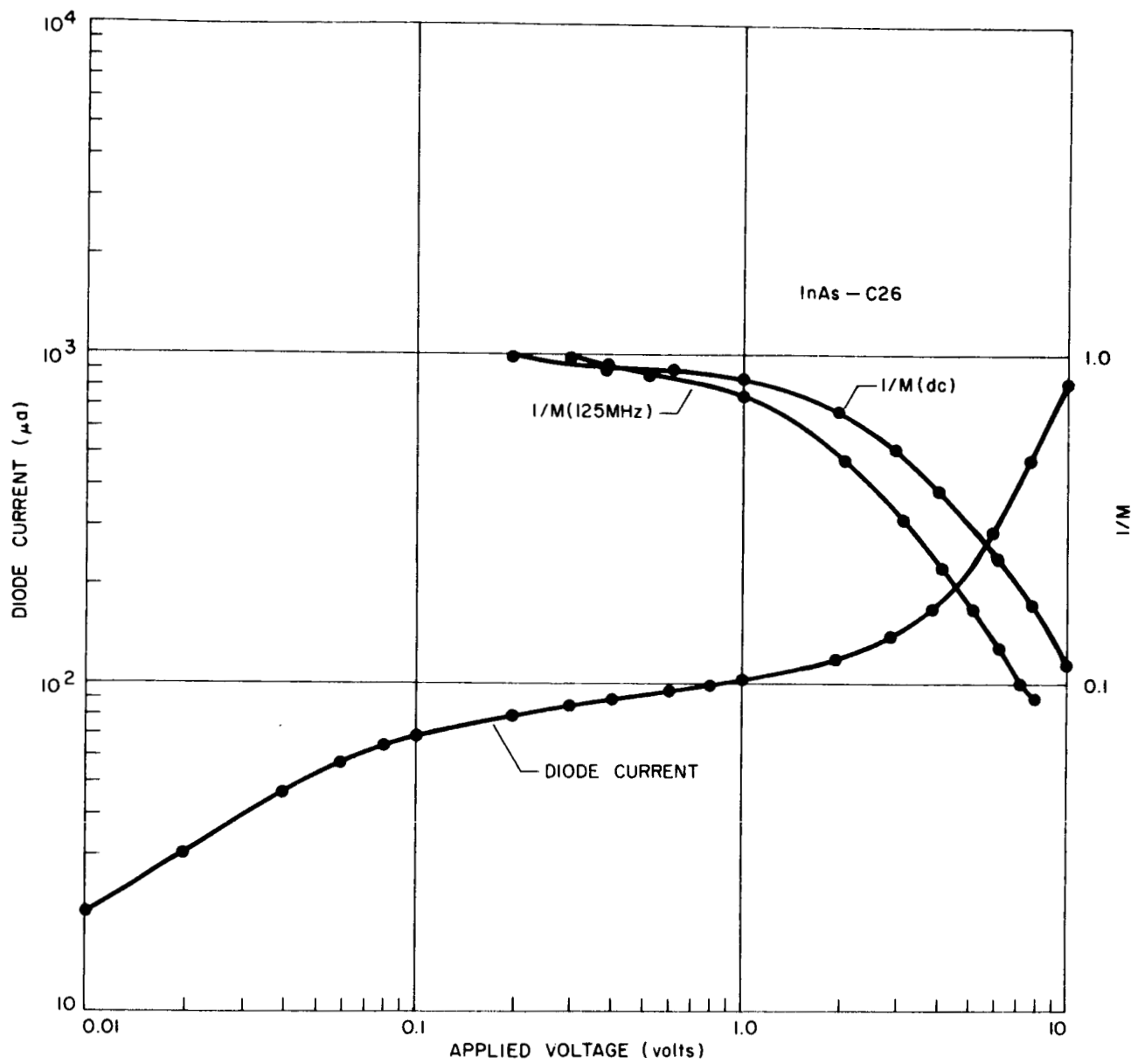


Figure 17. Reverse Bias Current-Voltage and Current Multiplication Characteristics for InAs-C26

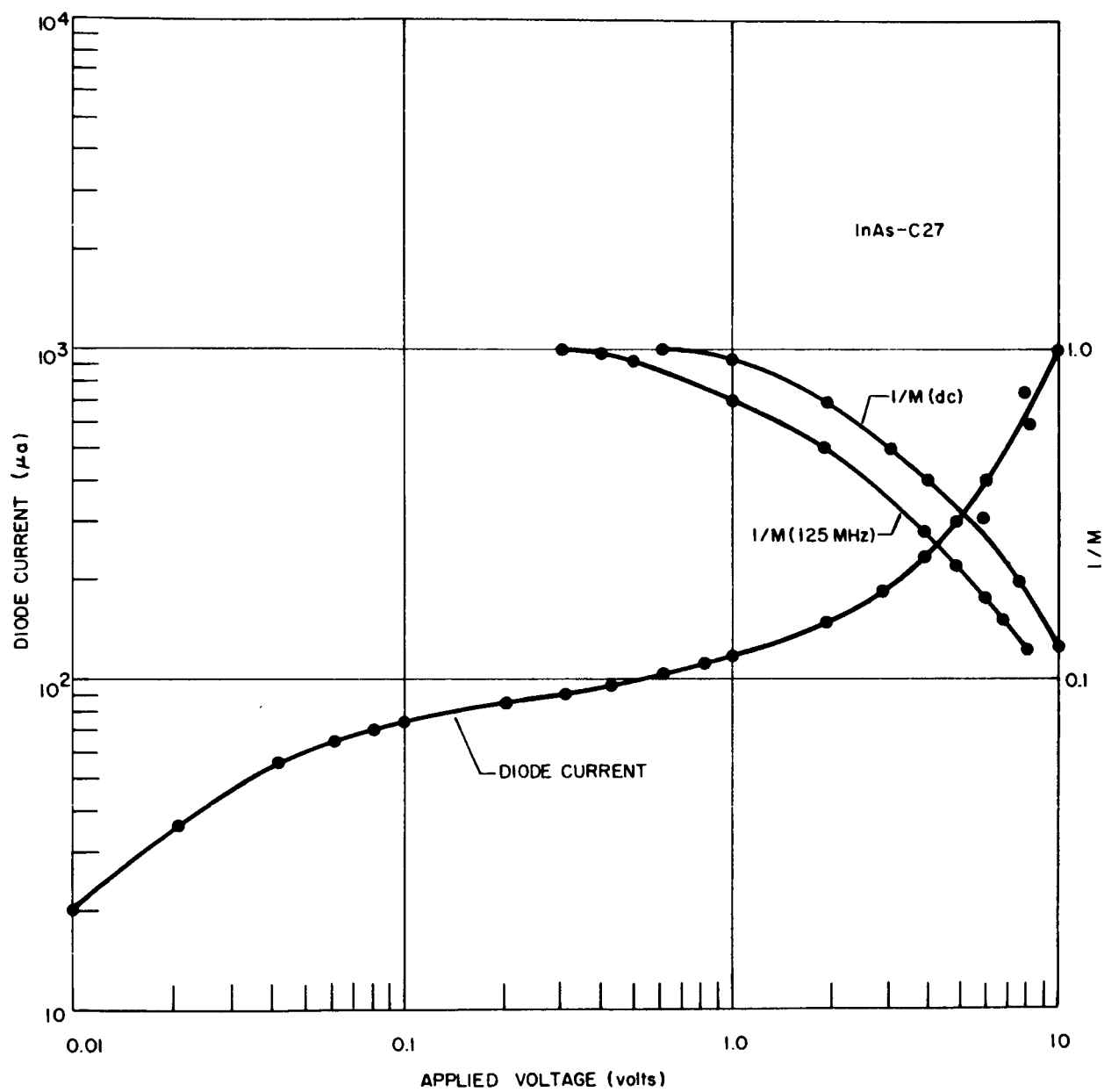


Figure 18. Reverse Bias Current-Voltage and Current Multiplication Characteristics for InAs-C27

be neglected at this temperature,²⁵ hence lack of saturation indicates a leakage resistance in parallel with the junction. The breakdown observed in all the diodes is soft. It is expected that a guard-ring-type structure would improve the diodes in both these respects. The current multiplication data has been obtained to 10 volts reverse bias in almost all cases, and the current multiplications observed at this bias voltage are between 8 and 12. The differences in the observed multiplications of some of the diodes at dc and at 125 MHz are most probably due to a slow shift in the diode current-voltage characteristic which occurs when the diodes are illuminated. This effect, which is seen in InSb photodiodes as well as in InAs photodiodes, is associated with the charging of slow surface states.

The sensitivity (D^*) of the InAs photodiodes to incoherent light was measured in order to establish that, in addition to providing current multiplication, the diodes were comparable in sensitivity to commercially available InAs photodiodes. The D^* measurements were made with a 500°K black body at 915 Hz, and the data was reduced to a 1-Hz bandwidth. The diodes were measured while reverse biased and drawing 50 μ A. The data is shown in Table 1. The average room temperature D^* is 0.9×10^8 which is within a factor of 2 to 3 of commercially available detectors. This data has been supplemented by the measurement of the spectral variation of the D^* in five cases. The spectral response curves are shown in Figure 19, and the D_λ^* at the wavelength of largest sensitivity is shown in Table 1. The series resistance R_s and junction capacitance C_j of the diodes, which limit their high-frequency performance, have been measured, and are given in Table 1. The series-resistance measurements were obtained from slotted-line reflectance measurements at 2 GHz. The capacitance data was obtained with a conventional capacitance bridge at 100 kHz. The computed $R_s C_j$ cutoff frequencies for the diodes range between 0.3 and 1.7 GHz. If the data is normalized to an area of 10^{-4} cm^2 , the cutoffs range from 1 to 5 GHz. Although the scatter is somewhat large, these values are in reasonable agreement with design expectations for diodes of this area.

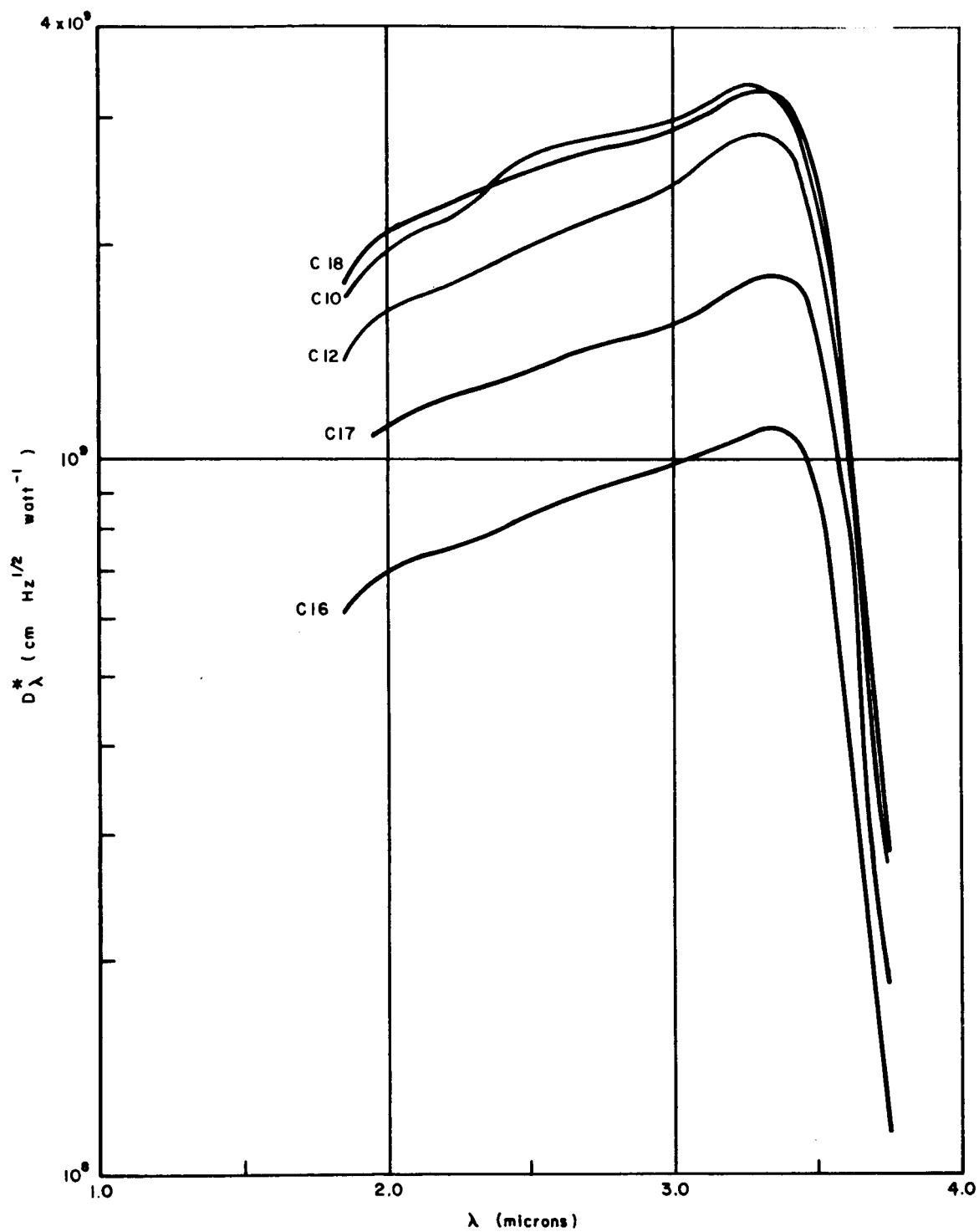


Figure 19. Spectral Sensitivities of Multiplying InAs Diodes

Table 1

Unit	R_s (ohms)	C_j (picofarads)	f_c (hertz)	Area ($\text{cm}^2 \times 10^{-4}$)	D^* (at 50 μa) ($\text{cm Hz}^{\frac{1}{2}} \text{ watt}^{-1}$)	D_λ^* peak (at 50 μa) ($\text{cm Hz}^{\frac{1}{2}} \text{ watt}^{-1}$)
C10	8.6	18.9	0.98	4.3	1.4×10^8	3.3×10^9
C12	8.8	17.7	1.0	2.4	1.1×10^8	2.8×10^9
C14	11.3	29.3	0.48	4.0	9.2×10^7	
C15	15.2	13.8	0.76	5.1	7.0×10^6	
C16	18.6	9.6	1.1	3.3	4.7×10^7	1.1×10^9
C17	9.8	14.4	1.1	3.8	7.5×10^7	1.8×10^9
C18	17.9	19.4	0.46	4.3	1.4×10^8	3.2×10^9
C19	14.6	9.8	1.1	3.3	5.4×10^7	
C20	14.9	31.1	0.34	2.8	7.1×10^7	
C21	10.4	48.0	0.32	3.8	1.5×10^8	
C22	17.2	25.7	0.36	10.5	1.8×10^8	
C23	13.2	7.1	1.7	3.0	4.1×10^7	
C24	21.8	11.7	0.62	7.3	8.3×10^7	
C25	10.4	13.3	1.2	4.6	1.4×10^8	
C26	18.6	11.6	0.74	6.8	7.8×10^7	
C27	33.5	11.0	0.43	7.2	9.1×10^7	

SECTION 3

CONCLUSIONS AND RECOMMENDATIONS

The theoretical work performed during this contract on the influence of current multiplication in avalanching diodes on diode bandwidth has been published.⁽¹⁶⁾ This work indicates that the ratio of the electron ionization coefficient (α) to the hole ionization coefficient (β) is important in determining the effect of multiplication on bandwidth. If $\beta/\alpha = 1$, the diode bandwidth decreases with multiplication. If $\beta/\alpha = 0$, the diode bandwidth is unaffected by multiplication. The excess current noise in avalanching diodes also depends critically on the ratio of the electron ionization coefficient to the hole ionization coefficient. If $\beta/\alpha = 0$, the signal and noise power are multiplied equally; if $\beta/\alpha > 0$, the noise power is multiplied more rapidly than the signal power. Thus, when $\beta/\alpha > 0$, avalanche multiplication results in a decrease in diode bandwidth and in diode signal-to-noise ratio. If in a particular case a photodiode is receiver noise-limited and has excess bandwidth, sufficient avalanche multiplication to overcome the receiver noise is useful; multiplication in excess of this amount is harmful.

It is recommended that further measurements of electron and hole ionization coefficients in common photodiode materials be undertaken. These constants are well known only in silicon. Further work is needed in germanium, and especially in III-V compounds, in order to determine more clearly to what extent bandwidth reduction and excess noise accompany avalanche multiplication.

The experimental effort to obtain a guard-ring structure in InAs during this program was unsuccessful. It is recommended that these studies be continued, in particular since better diffusion techniques in III-V compounds are now available. It is believed that improved diode reverse characteristics and enhanced multiplication will result. Following this work, the improvement of the crystalline perfection of the InAs starting material, through use of epitaxial techniques should provide further improvement in diode multiplication.

The mesa type InAs diodes made during the course of this work are consistent with the present state of the art. Current multiplications of 10 were obtained in these diodes at reverse biases of 10 volts. The RC cutoffs of these diodes are between 0.3 and 1.7 GHz. These cutoff frequencies are consistent with the diode areas of 2.4 to $10.0 \times 10^{-4} \text{ cm}^2$. Photodiodes with

RC cutoffs to at least 5 GHz can be made using the same techniques by reducing the diode area. Improvement in the current multiplication appears to depend on the development of diodes with more uniform breakdown characteristics.

SECTION 4

LIST OF PUBLICATIONS

R. B. Emmons and G. Lucovsky, "The Frequency Response of
Avalanching Photodiodes," IEEE Trans. ED-13, 297-305, (March 1966).

REFERENCES

1. K. M. Johnson, "Photodiode Signal Enhancement Effect at Avalanche Breakdown Voltage," ISSCC Digest of Tech. Papers, pp. 64-65 (Feb. 1964).
2. K. M. Johnson, "High-Speed Photodiode Signal Enhancement at Avalanche Breakdown Voltage," Trans. IEEE on ED 12, pp. 55-63 (Feb. 1965).
3. L. K. Anderson, P. G. McMullin, L. A. D'Asara, and A. Goetzberger, "Microwave Photodiodes Exhibiting Microplasma-Free Carrier Multiplication," Applied Physics Letters 6, 62-64 (1965).
4. A. S. Tager, "Current Fluctuations in a Semiconductor (Dielectric) Under the Conditions of Impact Ionization and Avalanche Breakdown," Soviet Physics - Solid State 6, pp. 1919-1925, (Feb. 1965).
5. R. J. McIntyre, "Avalanche Multiplication Noise in Semiconductor Junctions," IEEE Solid State Device Research Conference, Princeton, N. J., June 21-23, 1965.
6. R. J. McIntyre, "Multiplication Noise in Avalanche Diodes," IEEE Trans. ED-13, 164-168, (1966).
7. H. Melchior and L. K. Anderson, "Noise in High Speed Avalanche Photodiodes" International Electron Devices Meeting, Washington, D.C., Oct. 21, 1965.
8. C. A. Lee, R. A. Logan, R. L. Batdorf, J. J. Kleimock, and W. Wiegman, "Ionization Rates of Holes and Electrons in Silicon," Phys. Rev. 134, A761-A773, (1964).
9. S. L. Miller, "Avalanche Breakdown in Germanium," Phys. Rev. 99, 1234-1241, (1955).
10. R. A. Logan and A. G. Chynoweth, "Charge Multiplication in GaP p-n Junctions," Jour. App. Phys. 33, 1649-1654, (May 1962).
11. R. A. Logan, A. G. Chynoweth and B. G. Cohen, "Avalanche Breakdown in GaAs p-n Junctions" Phys. Rev. 128, 2518-2523, (1962).

12. H. Ruegg, "A Fast, High-Gain Silicon Photodiode," ISSCC Digest of Tech Papers, pp. 56-57, (Feb. 1966).
13. C. A. Lee and R. L. Batdorf, "Some Design Considerations for Multiplying Photodiodes," IEEE Solid State Device Research Conference, Boulder, Colo., July 1964.
14. W. T. Read, "A Proposed High Frequency Negative Resistance Diode," BSTJ. 37, 401-446, (1958).
15. G. Lucovsky and R. B. Emmons, "Avalanche Multiplication in InAs Photodiodes," ISSCC Digest of Tech Papers, pp. 52-53, (Feb. 1965).
16. R. B. Emmons and G. Lucovsky, "The Frequency Response of Avalanche Photodiodes," IEEE Trans. ED-13, 297-305, (March 1966).
17. B. W. Batterman, "X-Ray Integrated Intensity of Germanium: Effect of Dislocations and Chemical Impurities," JAP 30, 508-513, (1959).
18. H. Holloway in "Uses of Epitaxial Films in Physical Investigations" ed. J.C. Anderson, Acad. Press, New York (1966).
19. "Uniform Silicon pn Junctions; I Broad Area Breakdown," R. L. Batdorf, A. G. Chynoweth, G. C. Docey, and P. W. Fay, JAP 31, 1153-1160 (July 1960).
20. "Avalanche Effects in Silicon pn Junctions; II Structurally Perfect Junctions," A. Goetzberger, B. McDonald, R. H. Haitz, and R. M. Scarlett, JAP 34, 1591-1600 (June 1963).
21. Diffusion and Solubility in InAs, E. Schillman in Compound Semiconductors Ed by R. K. Willardson and H. L. Goering, Vol. 1, pp. 358-361, Reinbold, N.Y., 1962.
22. L. L. Chang, Solid State Elec. 7, 853
23. "Use of Low Temperature Deposited SiO₂ Films as Diffusion Masks in GaAs," W. S. Ing and W. Davern, Jour. Electrochem Soc. 111, 120-122 (Jan. 1964).
24. "Diffusion in III-V Compounds," D. L. Kendall, Thesis, Stanford Univ. Dept. of Materials Science, Aug. 1965, SU-DMS Report No. 65-29.
25. "Electrical Characteristics of Diffused InAs pn Junctions," G. Lucovsky, Brit. Jour. App. Physics 12, pp. 311-312 (June 1961).